



**HAL**  
open science

## Measuring the complex recombination dipole of aligned CO<sub>2</sub> molecules in high-order harmonic generation

Stefan Haessler, Willem Boutu, Hamed Merdji, Pierre Breger, Richard Taïeb,  
Jérémy Caillat, Alfred Maquet, Patrick Monchicourt, Bertrand Carré, Pascal  
Salières

► **To cite this version:**

Stefan Haessler, Willem Boutu, Hamed Merdji, Pierre Breger, Richard Taïeb, et al. (Dir.). Measuring the complex recombination dipole of aligned CO<sub>2</sub> molecules in high-order harmonic generation. pp.65 - 70, 2009, U VX 2008, 10.1051/uvx/2009011 . hal-01164785

**HAL Id: hal-01164785**

**<https://ensta-paris.hal.science/hal-01164785>**

Submitted on 18 Jun 2015

**HAL** is a multi-disciplinary open access archive for the deposit and dissemination of scientific research documents, whether they are published or not. The documents may come from teaching and research institutions in France or abroad, or from public or private research centers.

L'archive ouverte pluridisciplinaire **HAL**, est destinée au dépôt et à la diffusion de documents scientifiques de niveau recherche, publiés ou non, émanant des établissements d'enseignement et de recherche français ou étrangers, des laboratoires publics ou privés.

# Measuring the complex recombination dipole of aligned CO<sub>2</sub> molecules in high-order harmonic generation

Stefan Haessler<sup>1</sup>, Willem Boutu<sup>1</sup>, Hamed Merdji<sup>1</sup>, Pierre Breger<sup>1</sup>, Richard Taïeb<sup>2,3</sup>, Jérémie Caillat<sup>2,3</sup>, Alfred Maquet<sup>2,3</sup>, Patrick Monchicourt<sup>1</sup>, Bertrand Carré<sup>1</sup>, and Pascal Salières<sup>1</sup>

<sup>1</sup> CEA Saclay, IRAMIS, Service des Photons, Atomes et Molécules, 91191 Gif-sur-Yvette, France

<sup>2</sup> UMPC Univ. Paris 06, UMR 7614, Laboratoire de Chimie Physique-Matière et Rayonnement, 11 rue Pierre et Marie Curie, 75231 Paris Cedex 05, France

<sup>3</sup> CNRS, UMR 7614, LCPMR F-75005 Paris, France

**Abstract** We generate high order harmonics in aligned CO<sub>2</sub> molecules and measure the spectral amplitudes and phases as a function of the alignment angle. We control the quantum interference occurring in the recombination of an ultrafast laser-driven electron wavepacket with the highest occupied molecular orbital of CO<sub>2</sub>. By comparing to the emission of the reference system krypton, we obtain an experimental measure of the complex recombination dipole matrix element between the CO<sub>2</sub> HOMO and a continuum state. The measured phase jump contains signatures of Coulombic wavepacket distortion.

## 1 Introduction

High order harmonic generation (HHG) occurs when a strong laser field tunnel ionizes an atom or molecule, creating an electron wavepacket of attosecond duration that is subsequently accelerated and driven back to the core by the laser field[1,2]. At recollision, there is a certain probability for recombination to the ground state, releasing the accumulated kinetic energy in the form of an attosecond burst of XUV light. In a multi-cycle laser field, this process is repeated every half-cycle leading to a train of attosecond pulses whose spectrum contains only the odd harmonics of the laser frequency. Molecules as a generating medium can be aligned in the laboratory frame and the XUV emission may be considered a signal originating from an electron scattering process probing the highest occupied molecular orbital (HOMO)[3]. In the pioneering theoretical work of Lein et al. [4], the time dependent Schrödinger equation (TDSE) was solved for H<sub>2</sub><sup>+</sup> and H<sub>2</sub> molecules in an intense, linearly polarized laser field. An amplitude minimum as well as a jump of the spectral phase was observed at positions in the HHG spectrum which depend on the molecule alignment angle and the internuclear distance. These essential features could be described by the very simple two-center interference model[4].

## 2 Theoretical description

For a laser field with linear polarization along the x axis, the emitted complex HHG amplitude  $S(\omega)$  is given by the Fourier transform  $\mathcal{F}$  of the molecular dipole acceleration [5]. The latter should be obtained as the expectation value of the dipole acceleration operator  $\hat{a}$  ('acceleration form'), so that

$$S(\omega) = \mathcal{F} [\langle \Psi(\mathbf{r}, t) | \hat{a} | \Psi(\mathbf{r}, t) \rangle]. \quad (1)$$

Here, atomic units are used and  $\Psi(\mathbf{r}, t) = \Psi_{\text{HOMO}}(\mathbf{r})e^{iI_p t} + \Psi_c(x, t)$  is the total electronic wavefunction in the single-active-electron model, composed of the bound part (first summand) and the continuum electron wavepacket  $\Psi_c(x, t) = \int dk \alpha(k) e^{i(kx - k^2/2t)}$ . Here, we assume the depletion of the bound part due to tunnel ionization to be negligible and the continuum can be approximated by plane waves.  $\omega$  is the frequency of the emitted high harmonic radiation,  $I_p$  is the ionization potential of the molecule and  $k$  is the wavenumber of the recolliding electron. The electron recollision direction is fixed along the  $x$  direction by the laser polarization.

Via the Ehrenfest theorem, one can replace  $\langle \hat{a} \rangle$  in Eq. 1 by  $d/dt \langle \hat{p} \rangle$  ('velocity form'), where  $\hat{p}$  is dipole velocity operator. Alternatively,  $\langle \hat{a} \rangle$  may be replaced by  $d^2/dt^2 \langle \hat{x} \rangle$ , where  $\hat{x}$  is the dipole moment operator ('length form'). The equivalence of these forms only holds if  $\Psi_c(x, t)$  were composed of exact continuum wavefunctions, i.e. eigenfunctions of the same Hamiltonian as the HOMO wavefunction. Within the plane wave approximation for the continuum, however, these three forms are not equivalent any more. The acceleration form should be preferred[6] but Chirilă et al. [7] showed that the velocity form yields very reliable results, while being easier and faster to evaluate than the acceleration form. We thus re-write Eq. 1:

$$S(\omega) = \mathcal{F} \left[ \frac{d}{dt} \left\langle \Psi(\mathbf{r}, t) \left| \hat{p} \right| \Psi(\mathbf{r}, t) \right\rangle \right], \quad (2)$$

where  $\hat{p} = -i\partial/\partial x$ .

Eq. 2 now consists of three summands: One proportional to  $\langle \Psi_{\text{HOMO}} | \hat{p} | \Psi_{\text{HOMO}} \rangle$ , a second one  $\propto \langle \Psi_c | \hat{p} | \Psi_c \rangle$  and a cross term  $\propto \langle \Psi_{\text{HOMO}} e^{iI_p t} | \hat{p} | \Psi_c \rangle + \text{c.c.}$ . The first of these vanishes for bound states with defined parity, which is the case for simple symmetric molecules such as  $\text{CO}_2$ . The second term can be neglected as it represents continuum-continuum transitions which will give very small contributions only. We thus consider only the third term. With the above expression for  $\Psi(\mathbf{r}, t)$  and Eq. 2, we obtain for  $\omega > 0$ ,

$$S(\omega) = -i2\pi\omega \alpha(k(\omega)) \left\langle \Psi_{\text{HOMO}}(\mathbf{r}) \left| \hat{p} \right| e^{ik(\omega)x} \right\rangle \quad \text{for} \quad \omega = \frac{k^2}{2} + I_p. \quad (3)$$

Considering a simple molecule whose HOMO can be written as an antisymmetric combination of two atomic orbitals:  $\Psi_{\text{HOMO}}(\mathbf{r}) \propto \Phi_0(\mathbf{r} - \mathbf{R}/2) - \Phi_0(\mathbf{r} + \mathbf{R}/2)$ , where  $\mathbf{R}$  is the internuclear distance vector. The recombination dipole matrix element then reads:

$$\left\langle \Psi_{\text{HOMO}}(\mathbf{r}) \left| \hat{p} \right| e^{ik(\omega)x} \right\rangle = k(\omega) \sin \left( k(\omega) \frac{R}{2} \cos \theta \right) \left\langle \Phi_0(\mathbf{r}) \left| e^{ik(\omega)x} \right\rangle, \quad (4)$$

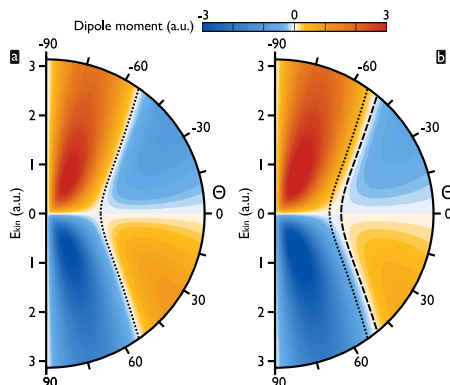
where  $\theta$  is the angle between the molecular axis and the electron wavevector given by the laser polarization. Obviously, destructive interference, i.e. a sign change of the recombination dipole matrix element, occurs for

$$R \cos \theta = n\lambda_e, \quad (5)$$

where  $n$  is an integer and  $\lambda_e$  is the electron de Broglie wavelength. The molecule then behaves like a two-point emitter whose emissions are dephased due to i) the path difference between the centers, ii) the symmetry of the orbital.

The  $\text{CO}_2$  molecule, although triatomic, is a good prototype for the two-center model as its HOMO is a  $\Pi$  orbital essentially formed by an anti-symmetric combination of two p orbitals centered on the oxygen atoms. We calculated the recombination dipole matrix element for the  $\text{CO}_2$  molecule using a HOMO wavefunction  $\Psi_{\text{HOMO}}$  computed with GAMESS (Hartree-Fock calculation). The result is shown in Fig. 1(b) together with lines marking the position of destructive interference according to Eq. 5. Agreement is obtained for a value of  $R = 3.9 a.u.$  which is smaller than the actual value of the distance between the two oxygen atoms  $R_{\text{O-O}} = 4.3 a.u.$ . We ascribe this deviation to the admixture to the HOMO of the  $d_{xy}$  ( $x$  along the internuclear axis) carbon orbital (7%), and also to a lesser extent of the  $d_{xy}$  oxygen orbitals (2%). The dipole contribution of the  $d_{xy}$  carbon orbital obviously does not present any interference. As for the  $d_{xy}$  oxygen orbitals, they contribute to the total HOMO as a symmetric combination and thus give rise to a destructive interference following:  $R \cos \theta = (n - 1/2)\lambda_e$ . The sum of these different terms leads to the observed deviation. In Fig. 1(a), only the p orbitals of the oxygen atoms are included, yielding perfect agreement with Eq. 5 for  $R = 4.3 a.u.$ .

**Figure 1. Theoretical dependence of the CO<sub>2</sub> recombination dipole on the angle and energy of the free electron plane wave.** Transition matrix element  $\langle \Psi_{\text{HOMO}} | \hat{p} | e^{ik(\omega)x} \rangle$ , shown in polar coordinates as a function of the angle  $\theta$  (deg) between the electron wavevector  $\mathbf{k}$  and the molecular axis, and the kinetic energy  $k^2/2$  (atomic units) of the electron at recollision. **(a)** In  $\Psi_{\text{HOMO}}$ , only the p orbitals of the oxygen atoms are included. The dipole moment changes sign when the recollision angle  $\theta$  follows equation 5 with  $n = 1$  and  $R = 4.3$  a.u. (dotted line). **(b)** Total  $\Psi_{\text{HOMO}}$  as computed with GAMESS (Hartree-Fock calculation). The prediction of Eq. 5 for  $R = 3.9$  a.u. is shown by the dashed line. (Figure taken from Ref. [8].)



### 3 Comparison of theoretical dipoles and experiment

To compare experimental results to the theoretical recombination dipole matrix elements shown in Fig. 1, it will be necessary to calibrate for  $\alpha(k)$  in Eq. 3. The authors of ref. [3] proposed to use a second measurement of  $S(\omega)$  under equal experimental conditions with a known reference system such as an atom with the same ionization potential as the molecule under study. This means that shape of the spectral amplitude  $\alpha(k)$  of the continuum electron wavepacket is assumed to depend mainly on the ionization potential and subsequent continuum dynamics governed by the laser field, and contains little information about the spatial structure of the bound state, i.e. the tunnel ionization process effectively acts as a strong spatial filter. We will only consider the  $\theta$ -dependence of the overall tunneling probability. For CO<sub>2</sub>, this reference atom is krypton:  $I_p(\text{Kr}) = 14.00$  eV,  $I_p(\text{CO}_2) = 13.77$  eV. Note that the  $S(\omega)$  as well as  $\alpha(k)$  are complex valued functions. Having measured the complex amplitudes  $S(\omega, \theta)_{\text{mol}}$  and  $S(\omega)_{\text{ref}}$  of the molecule and reference atom, respectively, Eq. 3 together with the assumption that  $\alpha(k)$  is the same for reference atom and molecule yields[8]:

$$\langle \Psi_{\text{HOMO}}(\theta) | \hat{p} | e^{ik(\omega)x} \rangle = \sqrt{\frac{P_{\text{ref}}}{P_{\text{mol}}(\theta)} \frac{|S_{\text{mol}}(\omega, \theta)|}{|S_{\text{ref}}(\omega)|}} e^{i[\varphi_{\text{mol}}(\omega, \theta) - \varphi_{\text{ref}}(\omega)]} \langle \Psi_{\text{ref}} | \hat{p} | e^{ik(\omega)x} \rangle \quad (6)$$

Here,  $\Psi_{\text{ref}}$  is the known 4p orbital of krypton,  $P_{\text{mol}}$  is the angle-dependent ionization yield of CO<sub>2</sub> and  $P_{\text{ref}}$  is the ionization yield of Kr. The recombination dipole matrix element can thus be extracted from the measured spectral amplitudes,  $|S_{\text{mol}}(\omega, \theta)|$  and  $|S_{\text{ref}}(\omega)|$ , and phases,  $\varphi_{\text{mol}}(\omega, \theta)$  and  $\varphi_{\text{ref}}(\omega)$ . The ionization yields could be measured in a separate experiment or calculated with ADK theory. Since the Kr dipole,  $\langle \Psi_{\text{ref}} | \hat{p} | e^{ik(\omega)x} \rangle$ , presents a smooth behaviour, the essential features of the CO<sub>2</sub> dipole,  $\langle \Psi_{\text{HOMO}}(\theta) | \hat{p} | e^{ik(\omega)x} \rangle$ , should directly show up in the experimental data. Note that the normalization of the CO<sub>2</sub> measurements by a krypton measurement under the same experimental conditions also corrects for the response of the experimental apparatus.

A second point to discuss here is the relation between the frequency  $\omega$  of the high order harmonic emission and that of the recolliding electron wavenumber  $k$ . Eq. 3 states  $\omega = k^2/2 + I_p$ , but often the heuristic relation  $\omega = k^2/2$  is used. The latter relation together with recombination dipole matrix elements in the velocity form predicts an interference position that agrees well with that obtained from TDSE simulations[9,10] for H<sub>2</sub><sup>+</sup>. It can be understood as a correction for the error induced by the plane wave approximation, which is valid only far away from the molecular potential. The acceleration of the recolliding electron by the molecular potential at the moment of recollision is approximately taken into account by increasing its energy by the amount of  $I_p$ , i.e. including it directly into  $k^2/2$  instead of adding it explicitly. In this paper, we follow this convention.

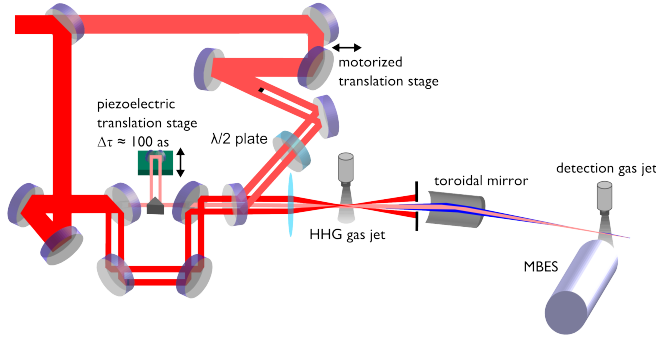


**Figure 2. Optical setup used for the experiments.** The laser beam enters at the upper left of the scheme. The part transmitted through the first beam splitter is the alignment beam. In the lower left part of the figure, the drilled mirror based interferometer for the RABITT[8,11,12] measurement is depicted. Here, the large annular beam is the harmonic generating beam, whereas the small central part is the probe pulse for RABITT. From the focusing lens on, the setup is placed under vacuum.

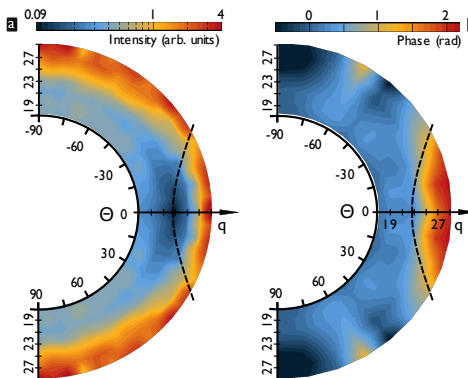
## 4 Experimental Setup and Methods

The experiments were carried out using the LUCA laser at CEA Saclay, delivering up 30mJ in 55 fs pulses at 20 Hz repetition rate. The setup is schematically shown in Fig. 2. A supersonic gas jet, whose temperature was estimated to  $\approx 90$  K, provides the molecular sample. We use the non-adiabatic alignment technique[13]: An alignment laser pulse focused to  $5 \times 10^{13} \text{ W/cm}^2$  creates a rotational wave packet in the medium through Raman excitation. Since the rotational frequencies of the excited rotational states are harmonics of a fundamental frequency, the wavepacket periodically rephases, resulting in an angular distribution of the molecular axis peaked along the polarization direction of the alignment laser pulse (confined in a cone angle of  $\sim 20^\circ$ ). The period of the rephasing is half the rotational period of the molecule, i.e. 21.1 ps for  $\text{CO}_2$ . This delay is set with a motorized translation stage and the molecule alignment angle  $\theta$  is set by controlling the polarization direction of the alignment pulse with a motorized half-wave plate. In the second arm, branched off at the first beam splitter, the Mach-Zehnder type interferometer for the RABITT[8,11,12] measurement is placed. Drilled mirrors separate the annular HHG beam (outer diameter cut to 17 mm by an iris), which contains most of the energy (typically 1 mJ), and the weak central part (typically 50  $\mu\text{J}$ , diameter  $\approx 4$  mm). The latter can be delayed by a piezoelectric translation stage with interferometric stability. In both arms, combinations of half-wave plate and polarizer allow to finely control the pulse energy. All three beams are then collinearly focused by the same lens of 1 m focal length  $\approx 5$  mm before the HHG gas jet. An iris then blocks the annular HHG beam and most of the alignment beam. The source of the high harmonic beam together with the on-axis probe beam are then imaged by a broad-band toroidal gold mirror into a magnetic-bottle electron spectrometer (MBES). In its interaction volume, the target gas neon, injected by a permanent leak, is photoionized by the high harmonics. The measurement of the photoelectron spectrum gives access to the spectral amplitudes  $|S(\omega)|$ . The presence of the weak IR probe pulse leads to the occurrence of spectral sidebands created by two-photon ionization involving a high harmonic photon and an IR photon. Analysis of these sidebands as a function of the probe beam delay gives access to the relative phase of two successive harmonic orders  $\phi_{q+2} - \phi_q$ , and thus to the group delay, also called *emission time*  $t_e$ [12]:

$$t_e(\omega_{q+1}) := \left. \frac{\partial \varphi}{\partial \omega} \right|_{q+1} \approx \frac{\phi_{q+2} - \phi_q}{2\omega_0}, \quad (7)$$

where  $\omega_0$  is the IR laser frequency. The sought-for spectral phase  $\varphi(\omega)$  can then be obtained at the discrete frequencies  $\omega_q = q\omega_0$  by integration of the emission time, up to a possibly  $\theta$ -dependent integration constant. In this paper, we assume that the phase of harmonic 15 generated in  $\text{CO}_2$  i) does not vary with angle, i.e. the integration constant is zero for all angles, and ii) for convenience, is the same as the one in Kr. The first assumption is supported by recent interferometric experiments[14].

**Figure 3. Experimental spectral intensity and phase of the CO<sub>2</sub> harmonic emission normalized by that of Kr.** CO<sub>2</sub> harmonic intensity and phase (measured for molecule angles from 90° to 0°) normalized to the krypton data taken under the same experimental conditions (intensity of  $0.95 \times 10^{14}$  W/cm<sup>2</sup>). In order to prevent the dispersion effects due to the larger ionization rate of Kr, the corresponding data were taken at lower pressure (25 Torr vs. 60 Torr for CO<sub>2</sub>) ensuring good phase matching conditions. The dashed lines are the same as the one shown in Fig. 1b converted to harmonic order. **(a)** Intensity ratio vs. alignment angle  $\theta$  (measured in steps of 5°) and harmonic order  $q$ . The ratio is not corrected for the different pressures. **(b)** Spectral phase difference (measured in steps of 10°).



## 5 Experimental Results

Using the RABITT[8,11,12] technique, we have measured amplitudes and phases of the high-order harmonic emission from aligned CO<sub>2</sub> molecules for harmonic orders 17 to 29 as a function of alignment angle  $\theta$ . The data are calibrated by a reference measurement with krypton according to the discussion on section 3, i.e. we calculate the difference of the spectral phases, shown in Fig. 3(b), and the ratio of the spectral intensities, shown in Fig. 3(a). Note that the latter quantity is the square of the ratio  $|S_{\text{mol}}|/|S_{\text{ref}}|$  appearing in Eq. 6.

As shown in Fig. 3, a clear intensity minimum is measured around harmonic 23 for  $\theta = 0^\circ$  that disappears when the molecule is rotated, and a phase jump of 2 rad is observed at the same position as the intensity minimum. Using the relation  $\omega = k^2/2$  (cp. sec. 3; the spectral range accessible in these experiments, harmonic 17 to 29, corresponds to electron energies of  $k^2/2 = 0.97$  to 1.65 a.u.), the position of these structures is the same as the position of the sign change of the theoretical recombination dipoles, shown in Fig. 1(b). The observed intensity minimum and phase jump are thus an experimental signature of two center quantum interference in the recombination dipole matrix element between the CO<sub>2</sub> HOMO and a continuum state.

There are, however, important deviations from the theoretical result, shown in Fig. 1(b). The theoretical dipole is purely real valued, i.e. its sign change corresponds to a step-like phase jump of  $\pi$ . In the experiment, the total phase jump is  $\approx 2.0$  rad, i.e. significantly smaller than  $\pi$  (value averaged over 8 measurements:  $2.0 \pm 0.6$  rad). Moreover, this jump is not step-like but spread over three harmonic orders. These deviations cannot be explained by an imperfect experimental alignment of the molecules: Convoluting the angular distribution with the dipole in Fig. 1(b) (both real-valued functions) would only induce a shift of the interference position but neither a spread nor a reduced value of the phase jump that both correspond to a complex dipole value. Such deviations appeared in early TDSE simulations[4] performed in H<sub>2</sub><sup>+</sup> and H<sub>2</sub> single molecules: A reduced phase jump of 2.7 rad spread over 5 orders was found in H<sub>2</sub><sup>+</sup> and even stronger deviations appeared in H<sub>2</sub>. A dipole calculation replacing the plane waves in equation 3 by two-center Coulomb wavefunctions has reproduced this behaviour[10]. Our measured phase jump would thus contain a direct signature of the Coulombic distortion of the recolliding electron wavepacket, uncovered by the high sensitivity of the quantum interference.

Finally, the theoretical recombination dipoles in Fig. 1(b) also change sign when at  $\theta = 0^\circ$  and  $\theta = 90^\circ$ . This is imposed by the  $\Pi$  symmetry of the CO<sub>2</sub> HOMO. There are two reasons why this sign change remains unseen in our experiments. First, we measure the derivative of the spectral phase,  $\varphi$ , with respect to the harmonic frequency,  $\omega$ , (cp. Eq. 7). This means that a change of the spectral phase that only depends on the angle  $\theta$  but not on  $\omega$  cannot be measured by the RABITT technique. This is why we could limit the scanned range to  $0^\circ \leq \theta \leq 90^\circ$  in our experiments. Second, the  $\Pi$  symmetry of the CO<sub>2</sub> HOMO results indeed in a quite different released electron wavepacket as compared to Kr close to  $\theta = 0^\circ$  and  $90^\circ$  with both a central

node and a change of sign. This sign change in the electron wavepacket will compensate the one of the orbital lobes and hence remove the sign change in the recombination dipole at  $\theta = 0^\circ$  and  $\theta = 90^\circ$ . The fact that the spectral intensity does not present a local minimum at  $\theta = 90^\circ$  but, on the contrary, is maximized, supports this interpretation.

## 6 Conclusions

In conclusion, we have presented an experimental measure of the complex valued recombination dipole matrix element  $\langle \Psi_{\text{HOMO}}(\theta) | \hat{p} | e^{ikx} \rangle$  between the CO<sub>2</sub> HOMO and the continuum state. Its essential features are understood by comparing to a simple model calculation. In particular an alignment angle dependent spectral minimum and phase jump can be described by a two-center interference model. Such a measurement is of great importance as benchmark for advanced models of molecules in strong laser fields. In particular we show that the plane wave approximation becomes questionable when a detailed description is needed. We did, however, show that the plane wave approximation still holds to the extent describing the essential structures of the experimental result. This is noteworthy, because the recombination dipole matrix element including plane waves can be read as a simple Fourier transform of the HOMO wavefunction, which, of course, opens exciting opportunities for imaging molecular orbital wavefunctions[3].

## References

1. P.B. Corkum, Physical Review Letters **71**(13), 1994 (1993)
2. K.J. Schafer, B. Yang, L.F. Dimauro, K.C. Kulander, Physical Review Letters **70**(11), 1599 (1993)
3. J. Itatani, J. Levesque, D. Zeidler, H. Niikura, H. Pepin, J. Kieffer, P. Corkum, D. Villeneuve, Nature **432**(7019), 867 (2004)
4. M. Lein, N. Hay, R. Velotta, J.P. Marangos, P.L. Knight, Phys. Rev. A **66**(2), 023805 (2002)
5. M. Lewenstein, P. Balcou, M.Y. Ivanov, A. L'Huillier, P.B. Corkum, Physical Review A **49**(3), 2117 (1994)
6. A. Gordon, F. Kartner, Physical Review Letters **95**(22), 223901 (2005)
7. C. Chirila, M. Lein, Journal of Modern Optics **54**(7), 1039 (2007)
8. W. Boutu, S. Haessler, H. Merdji, P. Breger, G. Waters, M. Stankiewicz, L. Frasninski, R. Taïeb, J. Caillat, A. Maquet et al., Nature Physics **4**(7), 545 (2008)
9. L. Kamta, A.D. Bandrauk, Phys. Rev. A **71**(5), 053407 (2005)
10. M.F. Ciappina, C.C. Chirila, M. Lein, Phys. Rev. A **75**(4), 043405 (2007)
11. P.M. Paul, E.S. Toma, P. Breger, G. Mullot, F. Auge, P. Balcou, H.G. Muller, P. Agostini, Science **292**(5522), 1689 (2001)
12. Y. Mairesse, A. de Bohan, L. Frasninski, H. Merdji, L. Dinu, P. Monchicourt, P. Breger, M. Kovacev, R. Taïeb, B. Carré et al., Science **302**(5650), 1540 (2003)
13. F. Rosca-Pruna, M.J.J. Vrakking, Physical Review Letters **87**(15), 153902 (2001)
14. Y. Mairesse, N. Dudovich, O. Smirnova, S. Patchkovski, D. Zeidler, J. Levesque, Y.M. Ivanov, D.M. Villeneuve, P.B. Corkum, *Interferometric measurements of molecular structure*, Talk at the "International workshop on Attosecond Physics", (2007)